

Fabrication and Properties of a Nanocomposite Multilayer Film Based on a Polyoxometalate

Jihong Liu^{a,b}, Tao Dong^b, Shuang Li^a, Huiyuan Ma^a, and Bo Liu^a

^a Key Laboratory of Green Chemical Engineering and Technology of College of Heilongjiang Province, College of Chemical and Environmental Engineering, Harbin University of Science and Technology, Harbin 150040, P. R. China

^b Chemistry Department, Harbin Normal University, Harbin 150025, P. R. China

Reprint requests to Huiyuan Ma. Tel.: 86-0451-86392716. Fax: 86-0451-86392716.

E-mail: mahy017@163.com or Bo Liu. E-mail: liubo200400@vip.sina.com.

Z. Naturforsch. **2012**, 67b, 673–677 / DOI: 10.5560/ZNB.2012-0102

Received April 12, 2012

A nanocomposite multilayer film based on a polyoxometalate $\text{Na}_{16}[\text{P}_4\text{W}_{30}\text{Mn}_4(\text{H}_2\text{O})_2\text{O}_{112}] \cdot x\text{H}_2\text{O}$ ($\text{Mn}_4\text{P}_4\text{W}_{30}$) was fabricated by the layer-by-layer self-assembly method. It was characterized by UV/Vis spectra and atomic force microscopy (AFM). The electrochromic and electrocatalytic properties were explored using chronoamperometry (CA), UV/Vis spectroscopy and cyclic voltammetry (CV). The attractive feature is a color change of the film by the reduction of the polyoxometalate at different potentials. The film also exhibits good electrocatalytic activity toward the reduction of IO_3^- .

Key words: Electrochromic Behavior, Layer-by-layer Deposition, Polyoxometalate, Electrocatalysis

Introduction

Polyoxometalates (POMs) have gained particular attention for their applications in many fields of science such as medicine, biology, catalysis, and materials due to their remarkable structural and electronic versatility. They show diverse properties such as catalytic activity for chemical transformations, molecule-based conductivity, magnetism, as well as photochromism, electrochromism, and luminescence [1–13]. One of the most important electronic properties of these structurally well defined polyoxometalate clusters is that they act as electron reservoirs since the reduction products are mixed-valence species with a characteristically deep-blue color (“heteropoly blues”) [14, 15]. As possible components of electrochromic devices, polyoxometalates (POMs) are promising candidates, also due to their ability to act as an electron reservoir, thereby giving rise to colored mixed-valent species while retaining their structural integrity [1, 16, 17]. In 1978, Tell and co-workers investigated the electrochromic properties of $\text{H}_3\text{PW}_{12}\text{O}_{40} \cdot 29\text{H}_2\text{O}$ and $\text{H}_3\text{PMo}_{12}\text{O}_{40} \cdot 29\text{H}_2\text{O}$ [18, 19], but these electrochromic cells have a disadvantage in that their

bleaching is slow when the color is intensified. Recently, Kurth *et al.* fabricated a multilayer film containing the POM cluster $[\text{Eu}(\text{H}_2\text{O})\text{P}_5\text{W}_{30}\text{O}_{110}]^{12-}$ by a layer-by-layer self-assembly method, which displayed good electrochromism [17]. Gao *et al.* prepared electrochromic multilayer films by the combination of a copper or an iron complex and a monolacunary Dawson-type polyoxometalate of P_2W_{17} . The color changes are adjustable depending on the extent of the reduction of the P_2W_{17} units, by applying more negative potentials [15], indicating that most POMs with a variety of structures could be investigated for practical applications in electrochromic materials.

Taking into account the above, we fabricated a nanocomposite multilayer film containing the polyoxometalate $\text{Na}_{16}[\text{P}_4\text{W}_{30}\text{Mn}_4(\text{H}_2\text{O})_2\text{O}_{112}] \cdot x\text{H}_2\text{O}$ ($\text{Mn}_4\text{P}_4\text{W}_{30}$) with electrochromic properties by the layer-by-layer self-assembly method. It was found that the multilayer film displays a color change from yellow to blue due to the reduction of the polyoxometalate. Also, their performance of higher contrast, suitable response time and low operation potential may be promising to meet the requirement for flexible displays and electrochromic devices.

Experimental

Materials

Tris(1,10-phenanthroline)ruthenium(II) chloride $\text{Ru}(\text{phen})_3\text{Cl}_2$, $\text{Ru}(\text{phen})_3$, polyethyleneimine (PEI MW 750,000), polystyrene sulfonate (PSS MW 70,000) and (3-aminopropyl)-trimethoxysilane were purchased from Aldrich Chemical Co. and used without further purification. The polyoxometalate $\text{Na}_{16}[\text{P}_4\text{W}_{30}\text{Mn}_4(\text{H}_2\text{O})_2\text{O}_{112}]\cdot x\text{H}_2\text{O}$ ($\text{Mn}_4\text{P}_4\text{W}_{30}$) was synthesized according to the literature procedure [20]. The water used in all experiments was deionized to a resistivity of $16\text{--}18\text{ M}\Omega\text{ cm}^{-1}$. All other reagents were of reagent grade.

Instrumentation

UV/Vis spectra of quartz-supported films were recorded on a U-3010 UV/Vis spectrophotometer made in Japan. All electrochemical experiments were carried out at a CHI 660B instrument at room temperature. A conventional three-electrode system was used, with a bare ITO electrode or a $\{\text{PSS}/\text{PEI}/[\text{Mn}_4\text{P}_4\text{W}_{30}/\text{Ru}(\text{phen})_3]_n\}$ multilayer film coated on an ITO electrode as a working electrode, platinum foil as a counter electrode, and Ag/AgCl as a reference electrode.

Preparation of the layer-by-layer film

Quartz substrates and ITO-coated glass were used for the preparation of the film by self-assembly. The substrates were cleaned according to the literature [21], which made their surface hydrophilic, rinsed with deionized water, and dried under a nitrogen stream. A precursor film was deposited on the hydrophilized substrate slide by immersing it into (3-aminopropyl)-trimethoxysilane, PSS and PEI solution for 20 min, respectively, followed by rinsing with deionized water and drying in a gentle nitrogen stream after each immersion. The precursor films were then alternately dipped into $2 \times 10^{-3}\text{ M}$ $\text{Mn}_4\text{P}_4\text{W}_{30}$ and $2 \times 10^{-3}\text{ M}$ $\text{Ru}(\text{phen})_3$ for 20 min. Deionized water-rinsing and nitrogen-drying steps were performed after each dipping. The multilayer film $\{\text{PSS}/\text{PEI}/[\text{Mn}_4\text{P}_4\text{W}_{30}/\text{Ru}(\text{phen})_3]_n\}$ was formed on the polymer matrix.

Results and Discussion

UV/Vis spectra

UV/Vis spectroscopy has proved to be a useful and facile technique to evaluate the growth process of multilayer films [22–25] and was used in the present work to monitor the assembling process of the $\{\text{PSS}/\text{PEI}/[\text{Mn}_4\text{P}_4\text{W}_{30}/\text{Ru}(\text{phen})_3]_n\}$ films. Fig. 1 shows the UV/Vis spectra of the

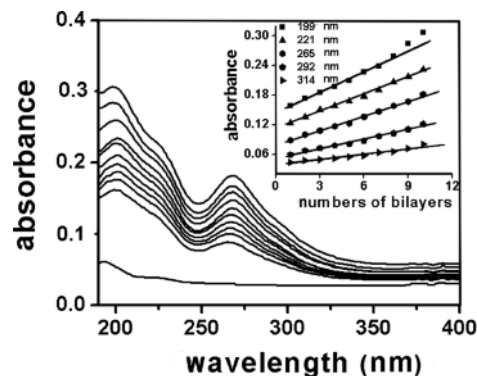


Fig. 1. UV/Vis spectra of multilayer films $\{\text{PSS}/\text{PEI}/[\text{Mn}_4\text{P}_4\text{W}_{30}/\text{Ru}(\text{phen})_3]_n\}$ ($n = 0\text{--}10$) deposited on quartz substrates (from bottom to top). Inset: The plots of the absorbance values at 199, 221, 265, 292, and 314 nm of the multilayer film ($n = 1\text{--}10$).

multilayer film $\{\text{PSS}/\text{PEI}/[\text{Mn}_4\text{P}_4\text{W}_{30}/\text{Ru}(\text{phen})_3]_n\}$ ($n = 0\text{--}10$) with $\text{Ru}(\text{phen})_3$ as the outermost layer. As shown in Fig. 1, the spectra showed five absorption peaks between 190 and 350 nm. The characteristic band at 292 nm is due to a ligand-centered $\pi\text{--}\pi^*$ transition, the bands centered at 221 and 314 nm are assigned to metal-centered $d\text{--}d$ transitions of the Ru cation [26–28]. The characteristic absorptions at 199 and 265 nm are attributed to the overlap peak of both $\text{Mn}_4\text{P}_4\text{W}_{30}$ and $\text{Ru}(\text{phen})_3$. The inset in Fig. 1 presents the plots of the absorbance values for these multilayer films at 199, 221, 265, 292, and 314 nm as a function of the number of deposition cycles. The absorbance values increase linearly with the number of $\text{Mn}_4\text{P}_4\text{W}_{30}/\text{Ru}(\text{phen})_3$ bilayers, indicating that a uniform multilayer film was fabricated.

Atomic force microscopy

The three-dimensional AFM image of the $\{\text{PSS}/\text{PEI}/[\text{Mn}_4\text{P}_4\text{W}_{30}/\text{Ru}(\text{phen})_3]_3\}$ film was taken to obtain detailed information about the surface morphology and the homogeneity of this deposited film. As seen in Fig. 2, a mass of uniform particles with a mean grain size of *ca.* 37 nm was observed on the surface of the film. The film presents a granular texture surface, with a root-mean-square roughness of 3.1 nm calculated over an area of $2.0 \times 2.0\text{ }\mu\text{m}^2$.

Electrochromic properties

The UV/Vis spectra of the $\{\text{PSS}/\text{PEI}/[\text{Mn}_4\text{P}_4\text{W}_{30}/\text{Ru}(\text{phen})_3]_{15}\}$ film modified on an

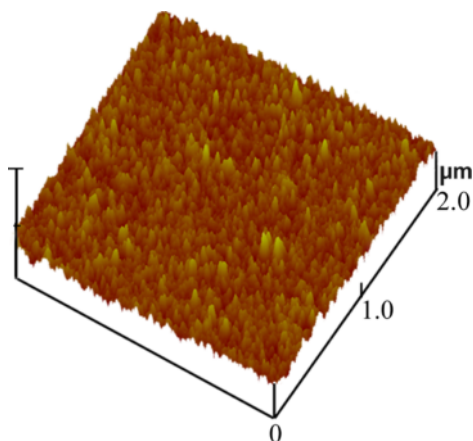


Fig. 2. A three-dimensional AFM image of a {PSS/PEI/[Mn₄P₄W₃₀/Ru(phen)₃]₃/Mn₄P₄W₃₀} film on silicon.

ITO electrode in 0.2 M NaAc + HAc (pH = 3.50) buffer solution were recorded under different potentials from 0 to −0.9 V (Fig. 3). When the applied potentials shifted toward negative, the absorbance at 567 nm was gradually increased, and the {PSS/PEI/[Mn₄P₄W₃₀/Ru(phen)₃]₁₅} film was gradually reduced to a different extent of green-blue color, which results from the charge transfer-type (W⁵⁺-O-W⁶⁺ or W⁶⁺-O-W⁵⁺) [15] optical absorption, indicating that the film was electrochromic. The response time of the film was investigated by double-potential experiments with absorbance measurements at 567 nm. The coloration and bleaching times are 5.5 and 7.0 s, respectively, for 90 % ΔA (difference

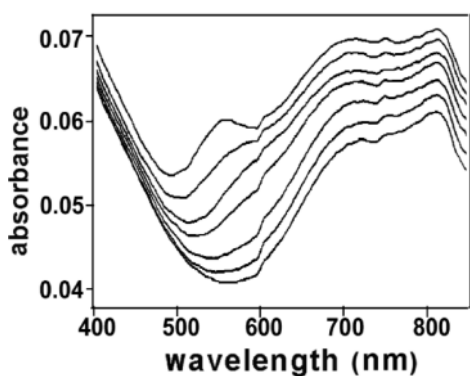


Fig. 3. UV/Vis spectra of the film {PSS/PEI/[Mn₄P₄W₃₀/Ru(phen)₃]₅/Mn₄P₄W₃₀} on an ITO electrode at different potentials. Bottom to top: 0, −0.4, −0.5, −0.6, −0.7, −0.8, and −0.9 V.

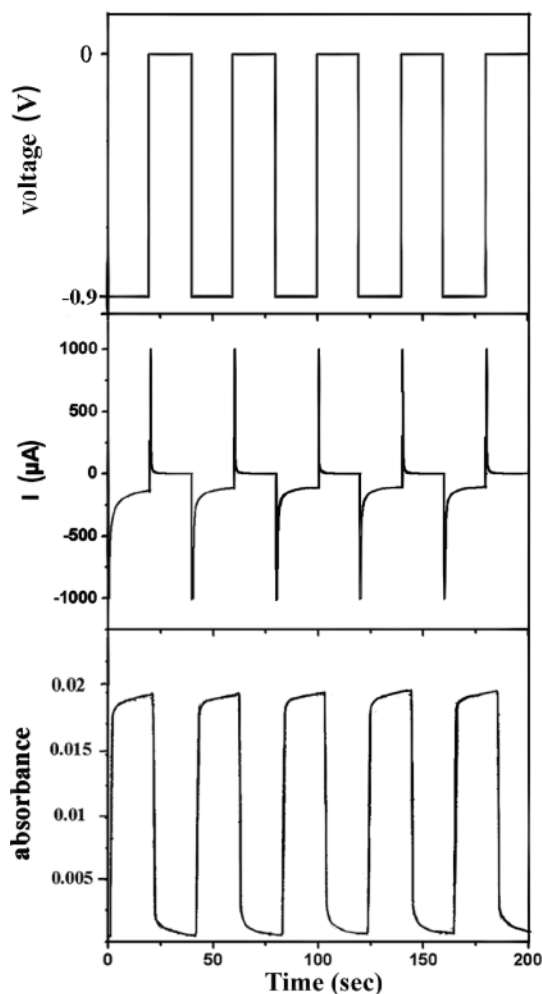


Fig. 4. Potential, current, and absorbance at 567 nm of a {PSS/PEI/[Mn₄P₄W₃₀/Ru(phen)₃]₅/Mn₄P₄W₃₀} -modified ITO electrode during subsequent double-potential steps (−900 to +500 mV).

between maxima) (see Fig. 4), which is faster than that of a similar [P₂W₁₇[Cu^{II}(Phen)₂]]₃₀ film previously reported by Gao (25 and 15 s for the coloration and bleaching times, respectively) [15]. At the same time, the electrochromic reversibility of the films was evaluated by performing repetitive double potential steps from −0.9 to 0 V (Fig. 4). The response time for coloration and bleaching as well as the absorbance of the electrochromic film did not change noticeably even after 200 cycles, which demonstrates a stable electrochromic behavior of the self-assembled films during double potential cycles.

Electrocatalytic activity

Our interest in the multilayer films is also related to its electrocatalytic behavior. Here, we use the {PSS/PEI/[Mn₄P₄W₃₀/Ru(phen)₃]₅/Mn₄P₄W₃₀} film as the working electrode, and iodate as the test species. Fig. 5 presents CVs of the multilayer film in 0.5 M Na₂SO₄ + H₂SO₄ (pH = 3.04) buffer solutions containing IO₃[−] at various concentrations. In the range −0.85 to 0.1 V, the cathodic peak currents of the three redox peaks of the {PSS/PEI/[Mn₄P₄W₃₀/Ru(phen)₃]₅/Mn₄P₄W₃₀} film increased substantially with the addition of iodate, while the relative anodic peak currents decreased, which indicated that iodate was reduced by four-electron, eight-electron, twelve-electron steps of Mn₄P₄W₃₀ [29]. The electrocatalytic efficiency can be calculated as defined by the equation [30]: $CAT = 100\% \times [I_p(POM, \text{substrate}) - I_p(POM)]/I_p(POM)$, where $I_p(POM, \text{substrate})$ and $I_p(POM)$ are the peak currents of the POM with and without the presence of substrate IO₃[−], respectively. When 0.6 mM IO₃[−] is employed, the electrocatalytic efficiency of the {PSS/PEI/[Mn₄P₄W₃₀/Ru(phen)₃]₅/Mn₄P₄W₃₀} film is 259%.

Conclusion

For the first time, the polyanion Mn₄P₄W₃₀ was incorporated into a multilayer film by a layer-by-layer self-assembly method, and the electrochromic properties of the film were investigated. This film exhibited electrochromism with good reversibility and stability.

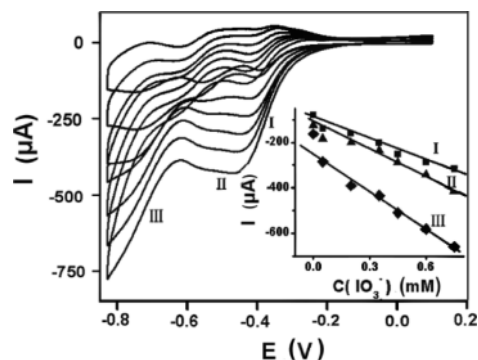


Fig. 5. CVs at an ITO/{PSS/PEI/[Mn₄P₄W₃₀/Ru(phen)₃]₅/Mn₄P₄W₃₀} multilayer film in 0.5 M Na₂SO₄+H₂SO₄ buffer solutions vs. Ag/AgCl (pH = 3.04) containing IO₃[−] in various concentrations. The inset shows the relationship between catalytic current and concentration of IO₃[−].

When more negative potentials were applied, the color of the film was gradually changed into deep blue. The coloration and bleaching times are 5.5 and 7.0 s, respectively, for 90% ΔA. This film also exhibited electrocatalytic activity toward iodate, and thus has the potential for application in electrochromic and electrocatalytic materials.

Acknowledgement

This work was financially supported by the National Science Foundation of China (no. 21071038 and 21101045), the Science and Technology Innovation Foundation of Harbin (no. 2010RFLXG004), the National Science Foundation of Heilongjiang Province (no. 201103), the Foundation of Educational Committee of Heilongjiang (no. 12511082, 12521072), and the Excellent Academic Leader Program of Harbin University of Science and Technology.

- [1] C. L. Hill, *Chem. Rev.* **1998**, *98*, 1.
- [2] E. Coronado, J. R. Galan-Mascaros, C. Gimenez-Saiz, C. J. Gomez-Garcia, *Adv. Mater.* **1993**, *4*, 283.
- [3] N. Casan-Pastor, L. C. W. Baker, *J. Am. Chem. Soc.* **1992**, *114*, 10384.
- [4] T. Yamase, *Mol. Eng.* **1993**, *3*, 241.
- [5] F. Bussereau, M. Picard, C. Malik, A. Teze, J. Blancou, *Ann. Inst. Pasteur/Virol.* **1988**, *32*, 33.
- [6] K. Ono, H. Nakane, F. Barre-Sinoussi, C. Chermann, *Nucleic Acids Res. Symp. Ser.* **1984**, *15*, 169.
- [7] M. Misono, *Catal. Rev. Sci. Eng.* **1987**, *29*, 269.
- [8] A. Watzenberger, G. Emig, D. T. Lynch, *J. Catal.* **1990**, *124*, 247.
- [9] M. T. Pope, A. Müller, *Angew. Chem., Int. Ed. Engl.* **1991**, *30*, 34.
- [10] M. T. Pope, *Heteropoly and Isopoly Oxometalates*, Springer, Berlin, **1983**.
- [11] M. T. Pope, A. Müller (Eds.), *Polyoxometalates: From Platonic Solids to Anti-Retroviral Activity*, Kluwer, Dordrecht, **1994**.
- [12] T. Shimidzu, A. Ohtami, M. Aiba, K. Honda, *J. Chem. Soc.* **1988**, *84*, 3941.
- [13] L. Ouahab, *Chem. Mater.* **1997**, *9*, 1909.
- [14] M. Clemente-León, E. Coronado, C. J. Gómez-García, C. Mingotaud, S. Ravaine, G. Romualdo-Torres, P. Delhaès, *Chem. Eur. J.* **2005**, *11*, 3979.

- [15] G. G. Gao, L. Xu, W. J. Wang, W. J. An, Y. F. Qiu, Z. Q. Wang, E. B. Wang, *J. Phys. Chem. B* **2005**, *109*, 8948.
- [16] J. C. Ma, D. A. Dougherty, *Chem. Rev.* **1997**, *97*, 1303.
- [17] S. Q. Liu, D. G. Kurth, H. Möhwald, D. Volkmer, *Adv. Mater.* **2002**, *14*, 225.
- [18] B. Tell, F. J. Wudl, *Appl. Phys.* **1979**, *50*, 5944.
- [19] B. Tell, S. Wagner, *Appl. Phys. Lett.* **1978**, *33*, 873.
- [20] R. G. Finke, M. W. Droge, P. J. Domaille, *Inorg. Chem.* **1987**, *26*, 3886.
- [21] I. Moriguchi, J. H. Fendler, *Chem. Mater.* **1998**, *10*, 2205.
- [22] F. Caruso, D. G. Kurth, D. Volkmer, M. J. Koo, A. Müller, *Langmuir* **1998**, *14*, 3462.
- [23] Y. H. Wang, X. L. Wang, C. W. Hu, C. S. Shi, *J. Mater. Chem.* **2002**, *12*, 703.
- [24] I. Ichinose, H. Tagawa, S. Mizuki, Y. Lvov, T. Kunitake, *Langmuir* **1998**, *14*, 187.
- [25] D. G. Kurth, D. Volkmer, M. Ruttorf, B. Richter, A. Müller, *Chem. Mater.* **2000**, *12*, 2829.
- [26] H. Y. Ma, J. Peng, Y. H. Chen, Y. H. Feng, E. B. Wang, *J. Solid State Chem.* **2004**, *177*, 3333.
- [27] N. Fay, E. Dempsey, A. Kennedy, T. McCormac, *J. Electroanal. Chem.* **2003**, *556*, 63.
- [28] J. E. Fergusson, G. M. Harris, *J. Chem. Soc. A* **1996**, *12*, 93.
- [29] L. Ruhlmanm, L. Nadjo, J. Canny, R. Contant, R. Thouvenot, *Eur. J. Inorg. Chem.* **2002**, *4*, 975.
- [30] M. Ammam, I.-M. Mbomekalle, B. Keita, L. Nadjo, J. Fransaer, *Electrochim. Acta* **2010**, *55*, 3118.